
Critical spin transport in Bose gases

Rakpong Kittinaradorn

July 22, 2011

Supervisors: Prof. Dr. Ir. H.T.C. Stoof
Dr. R.A. Duine



Universiteit Utrecht

Master Thesis
Institute for Theoretical Physics
Utrecht University

Critical spin transport in Bose gases

R. Kittinaradorn, R.A. Duine, and H.T.C. Stoof
*Institute for Theoretical Physics, Utrecht University,
 Leuvenlaan 4, 3584 CE Utrecht, The Netherlands*
 (Dated: July 22, 2011)

We consider spin transport in a two-component atomic Bose gas in three dimensions, at temperatures just above the critical temperature for Bose-Einstein condensation. In these systems the spin conductivity is determined by spin drag, i.e., frictional drag between the two spin components due to interactions. We find that in the critical region the temperature dependence of the spin conductivity deviates qualitatively from the Boltzmann result and is fully determined by the critical exponents of the phase transition. We discuss the size of the critical region where these results may be observed experimentally.

I. INTRODUCTION AND MOTIVATION

The research field of spin electronics or spintronics, concerned with practical applications of the electron spin, has renewed interest in spin currents¹. In part as a result of these efforts, it is now understood that there are several fundamental differences between charge currents and currents of spin angular momentum. For example, the latter are even under time reversal-symmetry operations and can thus in principle flow without dissipation in ordinary conductors^{2,3}, contrary to electric currents. Furthermore, the charge conductivity is infinitely large in Galilean invariant systems, whereas spin currents can then still decay due to spin-drag effects, i.e., friction between two spin states due to interactions^{4,5}. Finally, spin and charge current couple in a completely different way to other degrees of freedom in the system, most notably order parameters such as the magnetization or a superconducting condensate. For example, a spin current can exert a so-called spin transfer torque on the magnetization of a ferromagnet⁷⁻¹⁰, a phenomenon that is currently intensively studied in part because of its promise for magnetic-memory applications. On a more fundamental level, there have been several studies on the interplay between spin currents and the critical fluctuations in the magnetization that occur close to the Curie temperature for the ferromagnetic phase transition¹¹. Such magnetic phase transitions form, together with superconducting phase transitions, the overwhelming majority of phase transitions occurring in electronic condensed-matter physics.

In this thesis we consider the effect of another phase transition, i.e., Bose-Einstein condensation, on spin transport. The system we consider is a spin mixture of trapped ultracold bosonic alkali atoms that differs in several important ways from electronic solid-state systems. First, the particles are bosons rather than fermions (electrons). Second, cold-atom systems are disorder free and hence the only contribution to the spin conductivity is the above-mentioned spin-drag effect. The atomic interactions which are responsible for this drag are short ranged as opposed to the Coulomb interactions between the electrons.

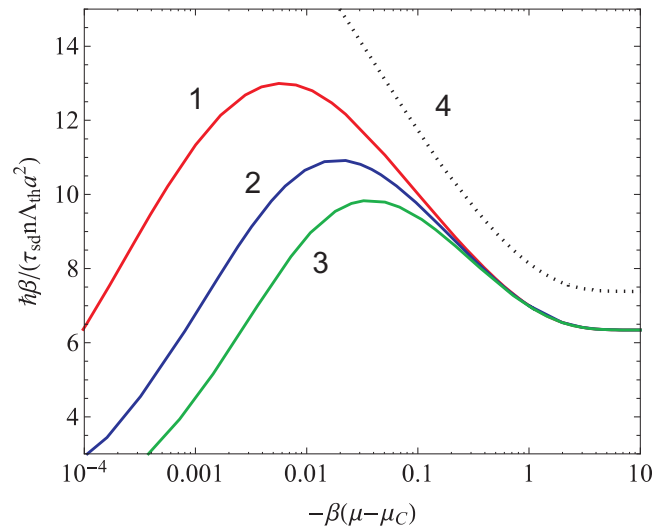


FIG. 1: (Color online) Spin-drag relaxation rate $1/\tau_{sd}$ at constant temperature as a function of distance from the critical point expressed in terms of the chemical potential difference $\mu - \mu_C$. Lines 1, 2 and 3 represent the relaxation rate for $a/\Lambda_{th} = 9 \times 10^{-3}$, $2(9 \times 10^{-3})$ and $3(9 \times 10^{-3})$, respectively, where a is the scattering length and $\Lambda_{th} = \sqrt{2\pi\hbar^2/(mk_B T)}$ is thermal de Broglie wavelength. Upon approaching the transition from above, the spin-drag relaxation rate shows an upturn due to Bose enhancement that is ultimately completely suppressed by fluctuations in the critical region. The dotted line 4 represents the Boltzmann result that does not include critical fluctuations¹⁷. The small quantitative difference between the lines 1-3 and the Boltzmann results far from criticality arises because we neglect vertex corrections in the calculations that lead to the curves 1-3.

Spin drag in bosonic cold-atom mixtures was recently studied by Duine and Stoof using an approach based on the Boltzmann equation. It was found that the bosonic nature of the particles lead to an enhancement of spin-drag effects at low temperatures¹². This should be contrasted with Fermi-liquid behavior that as a result of Pauli blocking leads to suppression of interaction effects at low temperatures so that the so-called spin-drag relaxation rate $1/\tau_{sd}(T)$, which is equal to the inverse of the

spin-transport relaxation time $\tau_{\text{sd}}(T)$, vanishes quadratically with temperature T ^{13,14} except in the vicinity of a superconducting¹⁵ or ferromagnetic phase transition¹⁶. For bosons close to the critical temperature for Bose-Einstein condensation, it was found that the Boltzmann approach incorporates the phase transition at the mean-field level and gives $1/\tau_{\text{sd}}(T) - 1/\tau_{\text{sd}}(T_C) \sim -1/\xi(T) \sim T_C - T$ ¹⁷, where $\xi(T)$ is the correlation length that diverges at the phase transition.

Our main findings are presented in Fig. 1 which shows the spin-drag relaxation rate as a function of the distance to the critical point, determined by the difference of the chemical potential μ from its critical value μ_C . The dotted line shows the Boltzmann result discussed in Chapter II (described above) and the solid lines are the results found using an approach based on the Kubo formula and approximating the atomic self-energy with the so-called sunset Feynman diagram shown in Fig. 8 and discussion in Chapter IV. The Hartree diagram should in principle also be included in the self-energy but since this can be achieved by a simple redefinition of the chemical potential we do not consider it here. Within the latter approximation we find that the spin-drag relaxation rate qualitatively agrees with the Boltzmann result for temperatures not too close to the critical temperature, but in the critical region deviates and goes to zero at the phase transition according to $1/\tau_{\text{sd}}(T) \sim 1/\xi(T)$. As we discuss in detail Chapter V, an exact scaling *ansatz* confirms that the spin-drag relaxation rate vanishes, and in terms of the critical exponents z , η , and ν we find that $1/\tau_{\text{sd}}(T) \sim 1/\xi^{z-d+2-2\nu}$. Below we also discuss the size of the critical region where these effects can be measured.

The above introduction is meant to give an overview of this paper. In the following two subsections, we will discuss spin transport and critical fluctuations in more details.

A. Spin transport and spin drag

Let us consider a system with two spin species under the external forces F_{\uparrow} and F_{\downarrow} . The equations of motion of each species are given by

$$\begin{aligned} n_{\uparrow} m_{\uparrow} \frac{dv_{\uparrow}}{dt} &= n_{\uparrow} F_{\uparrow} - \frac{n_{\uparrow} m_{\uparrow}}{\tau_{\text{sd}}} (v_{\uparrow} - v_{\downarrow}) - \frac{n_{\uparrow} m_{\uparrow}}{\tau_{\uparrow}} v_{\uparrow} \\ n_{\downarrow} m_{\downarrow} \frac{dv_{\downarrow}}{dt} &= n_{\downarrow} F_{\downarrow} + \frac{n_{\downarrow} m_{\downarrow}}{\tau_{\text{sd}}} (v_{\uparrow} - v_{\downarrow}) - \frac{n_{\downarrow} m_{\downarrow}}{\tau_{\downarrow}} v_{\downarrow}. \end{aligned} \quad (1)$$

Here the density, mass and drift velocity for spin up (down) atoms are denoted by n_{\uparrow} (n_{\downarrow}), m_{\uparrow} (m_{\downarrow}) and v_{\uparrow} (v_{\downarrow}), respectively. The important quantities for transport are the relaxation times τ_{\uparrow} , τ_{\downarrow} and τ_{sd} . The first two τ_{\uparrow} (τ_{\downarrow}) are the relaxation times for the particle currents $j_{\uparrow} = n_{\uparrow} v_{\uparrow}$ ($j_{\downarrow} = n_{\downarrow} v_{\downarrow}$). The mechanisms related to this relaxation can be the collision between atoms and impurities and/or phonons in case of high enough temperature. The last relaxation time τ_{sd} is associated with the

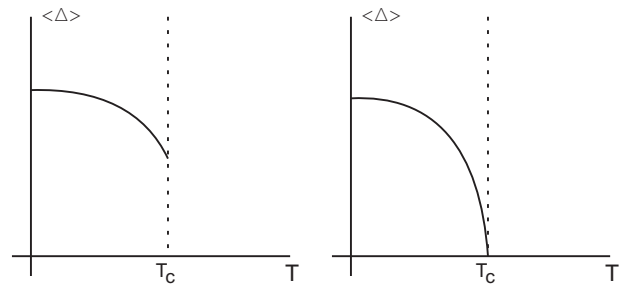


FIG. 2: Left: The order parameter jumps from zero to a finite value at the critical temperature for first-order phase transitions. Right: The order parameter changes continuously at the critical temperature for second-order phase transitions.

spin current ($j_s = n_{\uparrow} v_{\uparrow} - n_{\downarrow} v_{\downarrow}$). The relaxation mechanism of spin current has, in addition to the above effects, also contributions from collisions between different spin species. Momentum exchange between different species slows the spin current and thus relaxes the system. The characteristic time of this relaxation is called spin-drag relaxation time τ_{sd} and the mechanism itself is called spin drag^{4,5}. The aim of transport studies is to calculate the associated relaxation time microscopically.

In this thesis, we consider cold-atom systems where it is possible to have clean system without any disorders. In this case, the resistivity associated with particle current is zero and the relaxation time is infinite. The only interesting quantity is the spin-drag relaxation time. In addition, we only consider the most balanced case $n = n_{\uparrow} = n_{\downarrow}$, $m = m_{\uparrow} = m_{\downarrow}$ and $F_{\uparrow} = -F_{\downarrow}$.

B. Phase transition and critical fluctuations

The main aim of this paper is to incorporate critical fluctuations effects on spin transport. In this subsection we will show explicitly what are critical fluctuations and why are they important near critical points. In order to explain this, we first give a short review on Landau theory of phase transitions with a focus on second-order phase transitions⁶.

A phase transition is the phenomenon that a system dramatically changes its properties when an external parameter (usually temperature) is tuned across some critical values. To describe this change, we often use a parameter that describes the changing nature of the system. This parameter is called the order parameter Δ . The order parameter is often zero on one side of phase transition and has finite value on another side. The point in the phase diagram where order parameter changes to nonzero values is called the critical point. Phase transitions can be categorized into two types, first-order and second-order phase transitions. First-order phase transitions have a jump in the order parameter from zero to a fi-

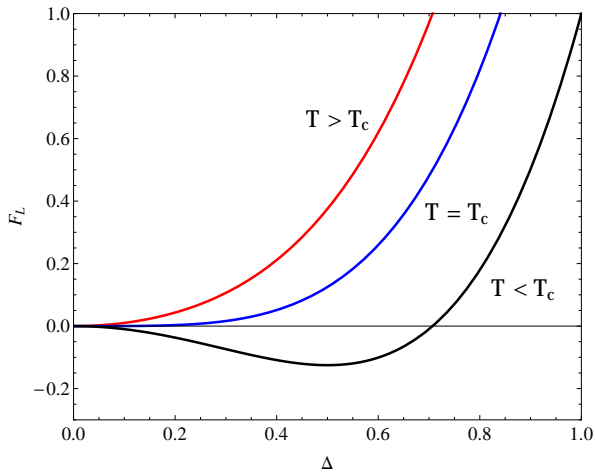


FIG. 3: (Color online) Landau free energy at various temperature. Below critical temperature, the minimum is shifted to nonzero order parameter.

nite value in a discontinuous way (Fig. 2 left). In second-order phase transitions the order parameter changes from zero to finite value in a continuous way (Fig. 2 right). We will emphasize on second-order phase transitions since Bose-Einstein condensation is of this type.

The standard approach to study second-order phase transition is the Landau theory of phase transition. The main quantity in this theory is the Landau free energy functional $F_L[\Delta]$ related to the partition function by

$$Z = \int d[\Delta] e^{-\frac{1}{k_B T} F_L[\Delta]} . \quad (2)$$

In order to describe the change of order parameter near critical point, we expand the free energy around small value of order parameter. Taking into account symmetries of the system such as rotational invariance, the Landau free energy can be expanded in the following form

$$F_L[\Delta] = \frac{1}{2} \int d\mathbf{x} \{ \gamma(T) (\nabla \Delta(\mathbf{x}))^2 + \alpha_1(T) \Delta(\mathbf{x})^2 + \frac{\alpha_2(T)}{2} \Delta(\mathbf{x})^4 + \dots \} . \quad (3)$$

To explain a continuous change of the order parameter near the critical point the quadratic coefficient has to change sign at the critical temperature (T_C) $\alpha_1(T) \approx \alpha_{1c} k_B (T - T_C)$ and the quartic coefficient has to be a constant $\alpha_2(T) \approx \alpha_{2c}$. The Landau free energy functionals with these coefficients are shown in Fig. 3 for various temperatures. The expectation value of the order parameter below the critical temperature can be calculated by minimizing the free energy $\delta F_L[\Delta] / \delta \Delta(\mathbf{x})|_{\Delta=\langle \Delta \rangle} = 0$. This gives the expectation value $\langle \Delta \rangle = \sqrt{\alpha_{1c} k_B |T - T_C| / \alpha_{2c}}$.

The above calculation of the order parameter has mean-field nature in the sense that critical fluctuations

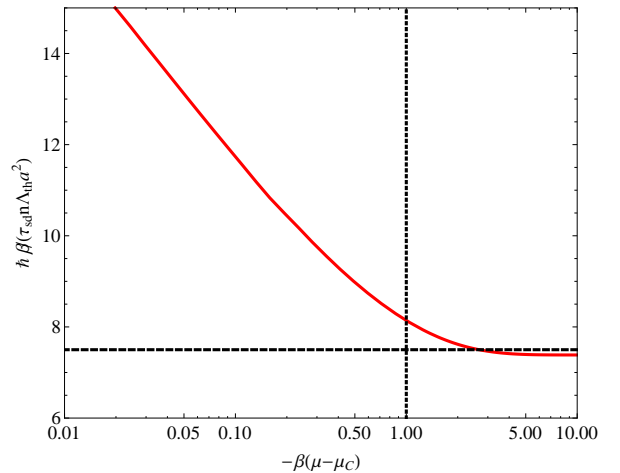


FIG. 4: (Color online) The solid line is spin-drag relaxation rate from Boltzmann calculation. The horizontal line is the analytic result in Maxwell-Boltzmann limit. The vertical line indicates $-\beta(\mu - \mu_C) = k_B T$ where Bose enhancement becomes important.

are not included. To study the effect of fluctuations, we write $\Delta(\mathbf{x}) = \langle \Delta \rangle + \Delta'(\mathbf{x})$. Plugging this into Eq. (3) we can calculate the correlation function of the fluctuations from the partition function. The correlation function in three dimensions is

$$\begin{aligned} \langle \Delta'(\mathbf{x}) \Delta'(\mathbf{x}') \rangle &= \frac{k_B T}{\gamma} \int \frac{d\mathbf{k}}{(2\pi)^3} \frac{e^{i\mathbf{k} \cdot (\mathbf{x} - \mathbf{x}')}}{\mathbf{k}^2 + \xi^{-1}(T)^2} \\ &= \frac{k_B T}{4\pi\gamma} \frac{e^{-|\mathbf{x} - \mathbf{x}'|/\xi(T)}}{|\mathbf{x} - \mathbf{x}'|} , \end{aligned} \quad (4)$$

where $\xi(T) = \sqrt{\gamma / |\alpha_1(T)|} \equiv |\mu - \mu_C|^{-\nu}$ is the correlation length of the fluctuations. Note that the correlation length diverges at the critical temperature as $\alpha_1(T)$ vanishes. These fluctuations are considered to be important if the Ginzburg criterion is satisfied

$$\langle \Delta'(\mathbf{x}) \Delta'(\mathbf{x}') \rangle > \langle \Delta \rangle^2 , \quad (5)$$

for the typical length scale $|\mathbf{x} - \mathbf{x}'| \approx \xi(T)$. Plugging in everything into Eq. (5), we find that critical fluctuations are important near the critical point where the expectation value of order parameter is small $\xi(T) > 4\pi\gamma^2 / (\alpha_{2c} k_B T_C)$. We note here that the Ginzburg criterion can be extended to the regime above critical temperature by replacing $\langle \Delta \rangle$ by $\langle |\Delta| \rangle$. The criterion for the correlation length is still the same up to an overall constant. The system becomes scale invariant near the critical point since the correlation length of the fluctuations diverges.

We can now put in the expansion coefficients for Bose-Einstein condensation. They are $\gamma = \hbar^2 / 2m$, $\alpha_1 =$

$-(\mu - \mu_C)$ and $\alpha_2/2 = 4\pi\hbar^2 a/m$, where μ and μ_C are chemical potential and critical chemical potential, respectively. Furthermore m is mass and a is the scattering length. The Ginzburg criterion then becomes $|\mu - \mu_C| < a^2$. Note that the exponent 2 is still mean-field exponent. We expect the critical exponent ν to be involved if fluctuations are incorporated more properly.

II. BOLTZMANN APPROACH AND COLLISION RATE

We consider a three-dimensional homogeneous gas of bosonic atoms of mass m , with two spin states that couple to an external force with opposite sign. As we discuss in more detail below, this force can in a cold-atom experiment be implemented by a magnetic-field gradient.

This force leads to a nonzero spin current \mathbf{j}_s according to $\mathbf{j}_s = \sigma_s \mathbf{F}$, where $\sigma_s = n\tau_{sd}/m$ is the spin conductivity in terms of the spin-drag relaxation time and the density n per spin state. The spin-drag relaxation rate $1/\tau_{sd}$ defined by the inverse of the relaxation time can be calculated straightforwardly by using Boltzmann equation^{12,17}. The starting point is two Boltzmann equations for two spin states

$$\begin{aligned} \frac{\partial f_{\uparrow}(\mathbf{k}, t)}{\partial t} + \frac{\mathbf{F}}{\hbar} \cdot \frac{\partial f_{\uparrow}(\mathbf{k}, t)}{\partial \mathbf{k}} &= \Gamma_{coll}(\mathbf{k}, t); \\ \frac{\partial f_{\downarrow}(\mathbf{k}, t)}{\partial t} - \frac{\mathbf{F}}{\hbar} \cdot \frac{\partial f_{\downarrow}(\mathbf{k}, t)}{\partial \mathbf{k}} &= -\Gamma_{coll}(\mathbf{k}, t), \end{aligned} \quad (6)$$

with the collision integral

$$\begin{aligned} \Gamma_{coll}(\mathbf{k}, t) &= \frac{2\pi}{\hbar} (T^{2B})^2 \int \frac{d\mathbf{k}_2}{(2\pi)^3} \int \frac{d\mathbf{k}_3}{(2\pi)^3} \int \frac{d\mathbf{k}_4}{(2\pi)^3} (2\pi)^3 \delta(\mathbf{k} + \mathbf{k}_2 - \mathbf{k}_3 - \mathbf{k}_4) \delta(\epsilon_{\mathbf{k}} + \epsilon_{\mathbf{k}_2} - \epsilon_{\mathbf{k}_3} - \epsilon_{\mathbf{k}_4}) \\ &\quad \times [f_{\uparrow}(\mathbf{k}_2) f_{\downarrow}(\mathbf{k}_2) (1 + f_{\downarrow}(\mathbf{k}_3)) (1 + f_{\uparrow}(\mathbf{k}_4)) - (1 + f_{\uparrow}(\mathbf{k})) (1 + f_{\downarrow}(\mathbf{k}_2)) f_{\downarrow}(\mathbf{k}_3) f_{\uparrow}(\mathbf{k}_4)], \end{aligned} \quad (7)$$

with $T^{2B} = 4\pi\hbar^2 a/m$ the two-body T matrix in terms of the interatomic scattering length a between the two spin states. The above equations can be solved by making an *ansatz* $f_{\alpha}(\mathbf{k}, t) = N_B(\epsilon_{\mathbf{k}} - mv_{\alpha}(t)/\hbar - \mu)$, where $\alpha \in \{\uparrow, \downarrow\}$ and $\epsilon_{\mathbf{k}} = \hbar^2 k^2/2m$. Furthermore, $N_B(x) = [e^{\beta x} - 1]^{-1}$ is the Bose-Einstein distribution function, with $\beta = 1/k_B T$ the inverse thermal energy. The assumption behind this *ansatz* is that the intra-species interaction equilibrates the system fast enough such that the system is always described by Bose-Einstein distribution. From the above Boltzmann equation it is found that¹⁷

$$\frac{1}{\tau_{sd}} = \frac{\hbar^2 \beta (T^{2B})^2}{6\pi n m} \int \frac{d\mathbf{q}}{(2\pi)^3} \int_{-\infty}^{\infty} d\omega q^2 \frac{\Im[\chi(\mathbf{q}, \omega)]^2}{\sinh^2(\beta\hbar\omega/2)}. \quad (8)$$

with

$$\Im[\chi(\mathbf{q}, \omega)] = \frac{m}{2\hbar^2 \Lambda_{th}^2 q} \ln \left[\frac{e^{\frac{q^2 \Lambda_{th}^2}{16\pi} - \beta\mu - \frac{\hbar\beta\omega}{2} + \frac{\pi(\hbar\beta\omega)^2}{q^2 \Lambda_{th}^2}} - e^{-\hbar\beta\omega}}{e^{\frac{q^2 \Lambda_{th}^2}{16\pi} - \beta\mu - \frac{\hbar\beta\omega}{2} + \frac{\pi(\hbar\beta\omega)^2}{q^2 \Lambda_{th}^2}} - 1} \right]. \quad (9)$$

The spin-drag relaxation rate can then be calculated numerically. The result is shown as the solid line in Fig. 4. The horizontal dashed line shows analytic result in Maxwell-Boltzmann limit. A small shift in this limit between analytic result and numerical result is numerical error. The vertical dotted line represents the value $-\beta\mu = k_B T$ where the result begins to deviate from Maxwell-Boltzmann limit. The temperature dependence in the Maxwell-Boltzmann limit can be understood by

a simple mean free path argument. The collision rate is proportional to the ratio between mean velocity and mean free path $1/\tau_{coll} \sim v/l$. Mean velocity will increase as $v \sim \sqrt{T}$ and mean free path is the inverse of density and square of scattering length $l = 1/4\pi a^2 n$. Here we have $1/\tau_{coll} n a^2 \sqrt{T} \sim \text{constant}$. The numerical result also gives the temperature dependence of spin-drag relaxation rate near phase transition $1/\tau_{sd}(T) - 1/\tau_{sd}(T_C) \sim T_C - T$. We note that critical fluctuations are not included here and the result will change qualitatively when we incorporate critical fluctuations, as we shall see in the next chapter.

A. Collision rate

Spin-drag relaxation rate should be compared with the collision rate between two spin states. The collision rate is calculated by

$$\begin{aligned} \frac{n}{\tau_{coll}} &= \frac{2\pi}{\hbar} (T^{2B})^2 \int \frac{d\mathbf{k}}{(2\pi)^3} \int \frac{d\mathbf{k}_2}{(2\pi)^3} \int \frac{d\mathbf{k}_3}{(2\pi)^3} \int \frac{d\mathbf{k}_4}{(2\pi)^3} (2\pi)^3 \\ &\quad \times \delta(\mathbf{k} + \mathbf{k}_2 - \mathbf{k}_3 - \mathbf{k}_4) \delta(\epsilon_{\mathbf{k}} + \epsilon_{\mathbf{k}_2} - \epsilon_{\mathbf{k}_3} - \epsilon_{\mathbf{k}_4}) N_B(\epsilon_{\mathbf{k}} - \mu) \\ &\quad \times N_B(\epsilon_{\mathbf{k}_2} - \mu) (1 + N_B(\epsilon_{\mathbf{k}_3} - \mu)) (1 + N_B(\epsilon_{\mathbf{k}_4} - \mu)). \end{aligned} \quad (10)$$

By going to center of mass frame, the above equation can be rewritten in a more suggestive form in terms of

the relative momentum distribution $f_{rel}(\mathbf{k})$,

$$\frac{1}{\tau_{coll}} = 4\pi a^2 \int \frac{d\mathbf{k}}{(2\pi)^3} \frac{\hbar k}{m} f_{rel}(\mathbf{k}). \quad (11)$$

In the Maxwell-Boltzmann limit, the relative momentum

distribution is just the Maxwell-Boltzmann distribution $f_{rel,MB}(\mathbf{k}) = \frac{1}{2\sqrt{2}} \exp[-\beta(\epsilon_{\mathbf{k}}/2 - \mu)]$. With Bose enhancement this distribution becomes

$$f_{rel}(\mathbf{k}) = \frac{1}{2n} \int_0^\infty \frac{dK}{(2\pi)^2} K^2 \int_{-1}^1 dv N_B \left(\epsilon_{\sqrt{K^2 + kKv + k^2/4}} - \mu \right) N_B \left(\epsilon_{\sqrt{K^2 - kKv + k^2/4}} - \mu \right) \times \int_{-1}^1 du \left[1 + N_B \left(\epsilon_{\sqrt{K^2 + kKu + k^2/4}} - \mu \right) \right] \left[1 + N_B \left(\epsilon_{\sqrt{K^2 - kKu + k^2/4}} - \mu \right) \right]. \quad (12)$$

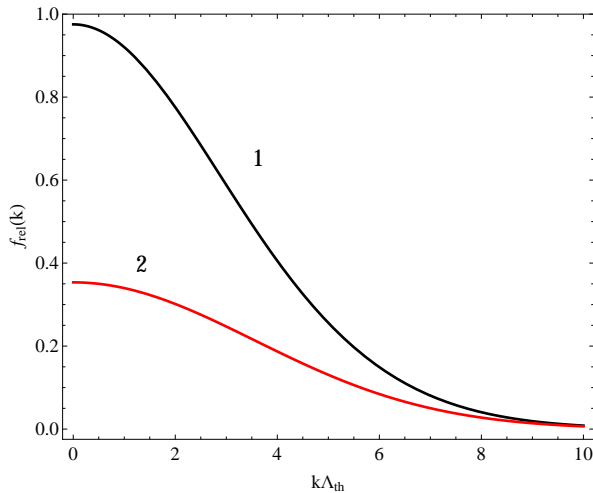


FIG. 5: (Color online) Relative momentum distribution with Bose enhancement (Line 1) and Maxwell-Boltzmann distribution (Line 2).

The result for this distribution together with its Maxwell-Boltzmann limit is shown in Fig. 5. Here we can see the effect of Bose enhancement on the relative momentum distribution. The collision rate is then calculated from this relative distribution. Fig. 6 (left) shows the effect of Bose enhancement on the collision rate. When comparing spin-drag relaxation rate with the collision rate, we can see from Fig 6 (right) that Bose enhancement is less efficient in spin-drag relaxation rate. Note that the ratio between spin-drag relaxation rate and collision rate in Maxwell-Boltzmann limit can be calculated analytically and is found as $1/\tau_{sd} = 2/3\tau_{coll}$.

III. FIELD THEORY APPROACH

We will incorporate critical fluctuations within a field theory framework. The goal is to find the spin current

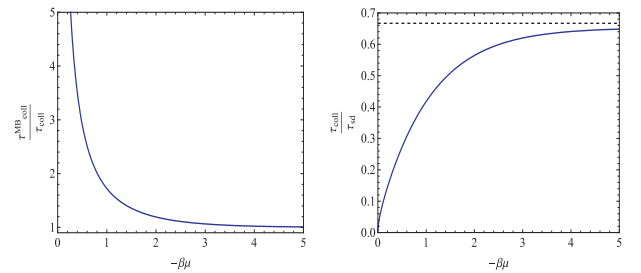


FIG. 6: Left: Ratio between the collision rate with and without Bose enhancement. Right: Ratio between spin-drag relaxation rate and collision rate. The horizontal line is $2/3$ the exact ratio in Maxwell-Boltzmann limit.

up to first order in the external force. The coefficient is then the spin conductivity. The starting point is the action $S = S_0 + S_{int}$ with the free part

$$S_0 = \int d\mathbf{x} \int d\tau \sum_{\alpha} \phi_{\alpha}^*(\mathbf{x}, \tau) \left[\hbar \frac{\partial}{\partial \tau} - \frac{\hbar^2 \nabla^2}{2m} - \mu \right] \phi_{\alpha}(\mathbf{x}, \tau). \quad (13)$$

We neglect interactions between atoms of like spins that are of minor importance for spin-drag effects. The interaction part of the action becomes

$$S_{int} = T^{2B} \int d\mathbf{x} \int d\tau \phi_{\uparrow}^*(\mathbf{x}, \tau) \phi_{\downarrow}^*(\mathbf{x}, \tau) \phi_{\downarrow}(\mathbf{x}, \tau) \phi_{\uparrow}(\mathbf{x}, \tau). \quad (14)$$

In the above expression the bosonic field is denoted by $\phi_{\alpha}(\mathbf{x}, \tau)$ with $\alpha \in \{\uparrow, \downarrow\}$ labeling the spin states. We add the force term by doing minimal coupling

$$-i\hbar\nabla \rightarrow -i\hbar\nabla - \frac{\alpha}{c} \mathbf{A}(\mathbf{x}, \tau). \quad (15)$$

We note that α takes the numerical value $+$ or $-$ for \uparrow and \downarrow respectively if it is not used as a label, $\mathbf{A}(\mathbf{x}, \tau)$ is

the vector potential to be related to external force. The action becomes $S = S_0 + S_{int} + S_F$ with the force term

$$S_F = - \int d\tau \int d\mathbf{x} \sum_{\alpha} \mathbf{A}(\mathbf{x}, \tau) \cdot \left\{ \frac{\hbar}{2mi} \frac{\alpha}{c} [\phi_{\alpha}^*(\mathbf{x}, \tau) \nabla \phi_{\alpha}(\mathbf{x}, \tau) - h.c.] - \frac{1}{2mc^2} \mathbf{A}(\mathbf{x}, \tau) \phi_{\alpha}^*(\mathbf{x}, \tau) \phi_{\alpha}(\mathbf{x}, \tau) \right\}. \quad (16)$$

The spin current is derived from the action by $\mathbf{J}(\mathbf{x}, \tau) = -c \frac{\delta S}{\delta \mathbf{A}(\mathbf{x}, \tau)}$. The spin current can be separated into two parts, paramagnetic and diamagnetic $\mathbf{J}(\mathbf{x}, \tau) = \mathbf{J}^p(\mathbf{x}, \tau) + \mathbf{J}^d(\mathbf{x}, \tau)$ where

$$\begin{aligned} \mathbf{J}^p(\mathbf{x}, \tau) &= \lim_{\mathbf{x}' \rightarrow \mathbf{x}} \sum_{\alpha} \frac{\alpha \hbar}{2mi} (\nabla_{\mathbf{x}'} - \nabla_{\mathbf{x}}) \phi_{\alpha}^*(\mathbf{x}, \tau) \phi_{\alpha}(\mathbf{x}', \tau) \\ \mathbf{J}^d(\mathbf{x}, \tau) &= \sum_{\alpha} \frac{1}{mc} \mathbf{A}(\mathbf{x}, \tau) \phi_{\alpha}^*(\mathbf{x}, \tau) \phi_{\alpha}(\mathbf{x}, \tau). \end{aligned} \quad (17)$$

The expectation value of an observable quantity $O(\mathbf{x}, \tau)$ can be calculated from the path integral formalism $\langle O \rangle = \frac{1}{Z} \int \mathcal{D}[\phi] O(\mathbf{x}, \tau) \exp(-S/\hbar)$, with $Z = \int \mathcal{D}[\phi] \exp(-S/\hbar)$ the partition function. In our case, the expectation value of spin current up to first order in the external force is given by

$$\begin{aligned} \langle J_{\mu}(\mathbf{x}, \tau) \rangle_{0, int, F} &= \\ \langle J_{\mu}^p(\mathbf{x}, \tau) \rangle + \langle J_{\mu}^d(\mathbf{x}, \tau) \rangle - \sum_{\nu} \int d\mathbf{x}' \int d\tau' & \\ \langle J_{\mu}^p(\mathbf{x}, \tau) J_{\nu}^p(\mathbf{x}', \tau') \rangle \frac{1}{\hbar c} A_{\nu}(\mathbf{x}', \tau'). & \end{aligned} \quad (18)$$

The subscript 0, *int*, *F* in the above expression means the average is taken with respect to $S_0 + S_{int} + S_F$. The average without subscript is taken in equilibrium (with respect to $S_0 + S_{int}$). The greek subscripts μ, ν denote the direction. The first term is actually zero in equilibrium. Recall that $\mathbf{E} = -\frac{\partial \mathbf{A}}{\partial t} + \nabla \psi$. We choose the gauge where $\psi = 0$ and $\mathbf{A}(\mathbf{x}, \tau) = -\frac{c\mathbf{E}}{\omega_p} e^{i\mathbf{k}\cdot\mathbf{x} - i\omega_p\tau} \equiv \frac{c}{\omega_p} \mathbf{F}(\mathbf{x}, \tau)$ with $\tau = -it$ the imaginary time and ω_p a bosonic matsubara frequency. The spin current becomes

$$\begin{aligned} \langle J_{\mu}(\mathbf{x}, \tau) \rangle_{0, int, F} &= \\ \sum_{\nu} \int d\mathbf{x}' \int d\tau' \left\{ -\frac{1}{m\omega_p} (n_{\uparrow} + n_{\downarrow}) \delta_{\mu\nu} \delta(\mathbf{x} - \mathbf{x}') \delta(\tau - \tau') \right. & \\ \left. - \frac{\Pi_{\mu\nu}(\mathbf{x} - \mathbf{x}', \tau - \tau')}{\omega_p} \right\} F_{\nu}(\mathbf{x}', \tau') & \\ \equiv \sum_{\nu} \int d\mathbf{x}' \int d\tau' \sigma_{\mu\nu}(\mathbf{x} - \mathbf{x}', \tau - \tau') F_{\nu}(\mathbf{x}', \tau'), & \end{aligned} \quad (19)$$

where $\Pi_{\mu\nu}(\mathbf{x} - \mathbf{x}', \tau - \tau') = \langle J_{\mu}^p(\mathbf{x}, \tau) J_{\nu}^p(\mathbf{x}', \tau') \rangle / \hbar$ the spin current spin current correlation function. Performing a

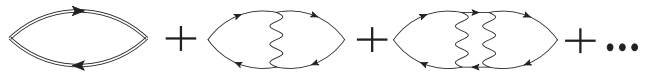


FIG. 7: Diagrammatic illustration of spin current spin current correlation function. The interacting Green function is denoted by a double line. The single line represents the non-interacting Green function. The first diagram is the most important. The rest are called vertex correction which we will ignore in this paper.

Fourier transform, we get the expression for conductivity

$$\sigma_{\mu\nu}(\mathbf{k}, i\omega_p) = -\frac{\Pi_{\mu\nu}(\mathbf{k}, i\omega_p)}{\hbar\omega_p} - \frac{1}{m\omega_p} (n_{\uparrow} + n_{\downarrow}) \delta_{\mu\nu}, \quad (20)$$

with $\Pi_{\mu\nu}(\mathbf{k}, i\omega_p)$ the fourier transform of $\Pi_{\mu\nu}(\mathbf{x} - \mathbf{x}')$. Eq.(20) is called Kubo formula. We can now do a Wick rotation $i\omega_p \rightarrow \omega_p^+ \equiv \omega_p + i\eta$ where η has infinitesimal positive value. Spin conductivity is obtained by taking the real part of above expression and take zero momentum zero frequency limit, $\sigma_s = -\lim_{\omega \rightarrow 0} \Im \left[\Pi_{\mu\nu}^{(+)}(\mathbf{k} = \mathbf{0}, \omega) \right] / \omega$, because we want to study time independent homogeneous systems.

The spin current spin current correlation function can be separated into two parts. They are illustrated diagrammatically in Fig. 7. The first diagram is the most important one in our system. The rest are called vertex correction which we will ignore in this thesis. We will come back to the validity of this approximation in the discussion section. Mathematically, ignoring vertex correction corresponds to making the approximation

$$\begin{aligned} \langle \phi_{\alpha}^*(\mathbf{x}, \tau) \phi_{\alpha}(\mathbf{x}'', \tau) \phi_{\alpha'}^*(\mathbf{x}', \tau') \phi_{\alpha'}(\mathbf{x}''', \tau') \rangle &= \\ \langle \phi_{\alpha}^*(\mathbf{x}, \tau) \phi_{\alpha}(\mathbf{x}'', \tau) \rangle \langle \phi_{\alpha'}^*(\mathbf{x}', \tau') \phi_{\alpha'}(\mathbf{x}''', \tau') \rangle & \\ + \langle \phi_{\alpha}^*(\mathbf{x}, \tau) \phi_{\alpha'}(\mathbf{x}''', \tau') \rangle \langle \phi_{\alpha'}^*(\mathbf{x}', \tau') \phi_{\alpha}(\mathbf{x}'', \tau) \rangle. & \end{aligned} \quad (21)$$

Thus the correlation function can be written in term of Green's function $G_{\alpha, \alpha'}(\mathbf{x}, \tau; \mathbf{x}', \tau') = -\langle \phi_{\alpha}(\mathbf{x}, \tau) \phi_{\alpha'}^*(\mathbf{x}', \tau') \rangle$. Upon ignoring vertex corrections to the correlation function $\Pi_{\mu\nu}^{(+)}(\mathbf{k}, \omega)$ and using the relation $G_{\alpha}(\mathbf{k}, i\omega_n) = -\hbar \int d\omega \rho_{\alpha}(\mathbf{k}, \omega) / (i\omega_n - \omega)$ the Kubo formula for the spin conductivity is worked out to yield

$$\sigma_s = -\frac{\pi \hbar^3}{3m^2} \sum_{\alpha \in \{\uparrow, \downarrow\}} \int \frac{d\mathbf{k}}{(2\pi)^3} k^2 \int d\omega \frac{dN_B(\hbar\omega)}{d\omega} \rho_{\alpha}^2(\mathbf{k}, \omega). \quad (22)$$

Given an approximation of the selfenergy, we can calculate the spectral function and spin-drag conductivity from the above equation by using also the Dyson equation $G(\mathbf{k}, i\omega_n) = \hbar / \{i\hbar\omega_n - [\epsilon_{\mathbf{k}} - \mu + \hbar\Sigma(\mathbf{k}, i\omega_n)]\}$. We will mainly discuss the sunset diagram for the selfenergy in this thesis. Improvement to the result of this thesis can be done straightforwardly by considering more involved diagrams. We also give another example of selfenergy in Appendix A.

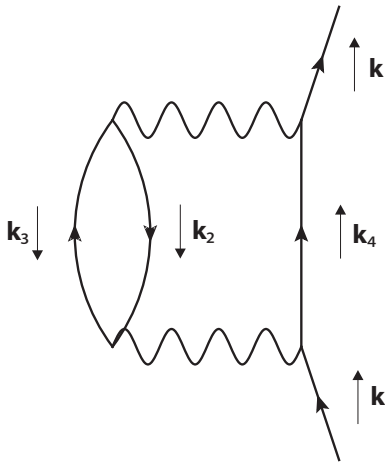


FIG. 8: Sunset diagram for the self-energy of spin-up particles (the diagram for spin-down is obtained by reversing all spins).

IV. SUNSET DIAGRAM

The lowest-order (in interatomic interactions) diagram that gives a finite conductivity is the sunset diagram in Fig. 8 for the atomic self-energy

$$\begin{aligned} \Im[\hbar\Sigma_{\alpha}^{(+)}(\mathbf{k}, \omega)] = & \\ & -\pi(T^{2B})^2 \int \frac{d\mathbf{k}_2}{(2\pi)^3} \int \frac{d\mathbf{k}_3}{(2\pi)^3} \int \frac{d\mathbf{k}_4}{(2\pi)^3} \\ & \times (2\pi)^3 \delta(\mathbf{k} + \mathbf{k}_2 - \mathbf{k}_3 - \mathbf{k}_4) \delta(\omega + \mu + \epsilon_{\mathbf{k}_2} - \epsilon_{\mathbf{k}_3} - \epsilon_{\mathbf{k}_4}) \\ & \times [N_B(\mathbf{k}_2)(1 + N_B(\mathbf{k}_3))(1 + N_B(\mathbf{k}_4)) \\ & - (1 + N_B(\mathbf{k}_2))N_B(\mathbf{k}_3)N_B(\mathbf{k}_4)]. \end{aligned} \quad (23)$$

The imaginary part of the self-energy is calculated numerically from Eq. (23). Its real part is obtained by using the Kramers-Kronig relation that holds for any complex function $\chi(\omega) = \chi_1(\omega) + i\chi_2(\omega)$ analytic in the upper half of complex frequency ω plane and vanishing faster than $1/|\omega|$ as $\omega \rightarrow \infty$. This relation is:

$$\begin{aligned} \chi_1(\omega) &= \frac{1}{\pi} \mathcal{P} \int_{-\infty}^{\infty} \frac{\chi_2(\omega')}{\omega' - \omega} d\omega' \\ \chi_2(\omega) &= -\frac{1}{\pi} \mathcal{P} \int_{-\infty}^{\infty} \frac{\chi_1(\omega')}{\omega' - \omega} d\omega'. \end{aligned} \quad (24)$$

Looking at the imaginary part of selfenergy in Fig.9 (left), we can see a problem at large frequency as it does not vanish. This problem can be circumvented by noting that the large frequency behaviour of the imaginary part goes like a square root of frequency. We can then calculate the corresponding real part of $\Im[\hbar\Sigma_{\alpha}^{(+)}(\mathbf{k}, \omega)] - A\sqrt{\omega}$ and subtract the square root part out of the result later to get the real part of the selfenergy (Fig.9 right), where A is a constant for a given momentum.

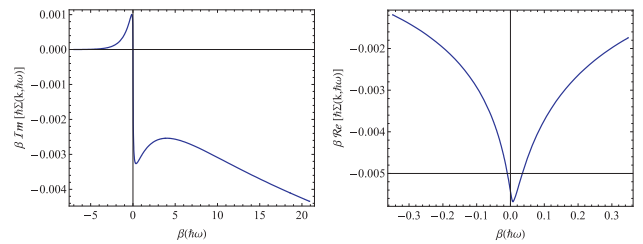


FIG. 9: Imaginary part(left) and real part(right) of the self-energy from sunset diagram at $\mathbf{k}\Lambda_{th} = 0.1$, $a/\Lambda_{th} = 9 \times 10^{-3}$ and $-\beta(\mu - \mu_C) = 0.1(a/\Lambda_{th})^2$.

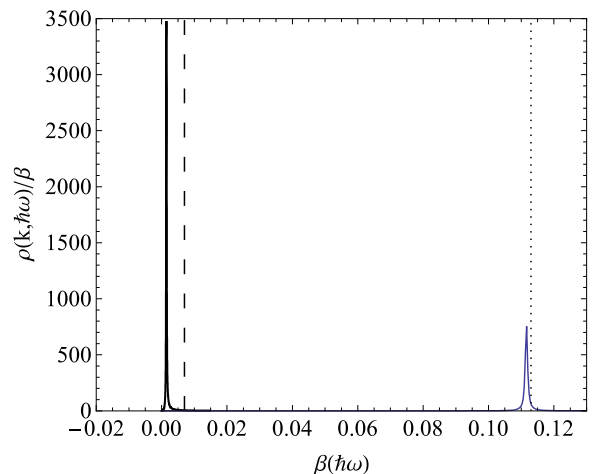


FIG. 10: The spectral function at low momentum inside (left) and outside (right) the critical region. The dashed and dotted lines show the value of $\epsilon_{\mathbf{k}} - \mu$ for the spectral function inside and outside the critical region, respectively.

This real part shifts the critical chemical potential from its noninteracting value of zero to the negative value $\mu_C = \Re[\hbar\Sigma^{(+)}(\mathbf{0}, 0)]$. We have checked that the frequency sum-rule $\int d\hbar\omega \rho_{\alpha}(\mathbf{k}, \omega) = 1$ which follows from the bosonic commutation relation is obeyed.

The result for the spectral function is shown in Fig. 10 as a function of frequency. For a given momentum, the spectral function exhibits a rather sharp Lorentzian peak corresponding to a quasi-particle excitation. For such a Lorentzian spectral function, the frequency integral in Eq. (22) can be performed and the resulting conductivity is then found to be proportional to the life-time $\tau(\mathbf{k}) = -\hbar/(2\Im[\hbar\Sigma^{(+)}(\mathbf{k}, \omega_{\mathbf{k}})])$ of the quasi-particle, where $\omega_{\mathbf{k}}$ is the solution of $\hbar\omega_{\mathbf{k}} = \epsilon_{\mathbf{k}} - \mu + \Re[\hbar\Sigma^{(+)}(\mathbf{k}, \omega_{\mathbf{k}})]$. The evaluation of the expression for the spin conductivity in Eq. (22) with the above expression for the self-energy leads to the results shown in Fig. 1 for various scattering lengths. The critical exponent is now changed into $\sigma_s \sim 1/\sqrt{\mu_C - \mu}$ (see Fig. 11).

Using this spectral function, we also calculate the shift

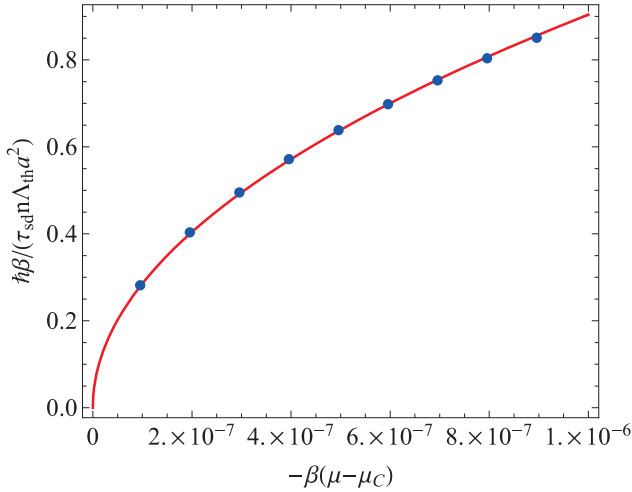


FIG. 11: Spin-drag relaxation rate near the critical point. The fitting line is $\hbar\beta/(\tau_{sd}n\Lambda_{th}a^2) = 900\sqrt{-\beta(\mu - \mu_C)}$.

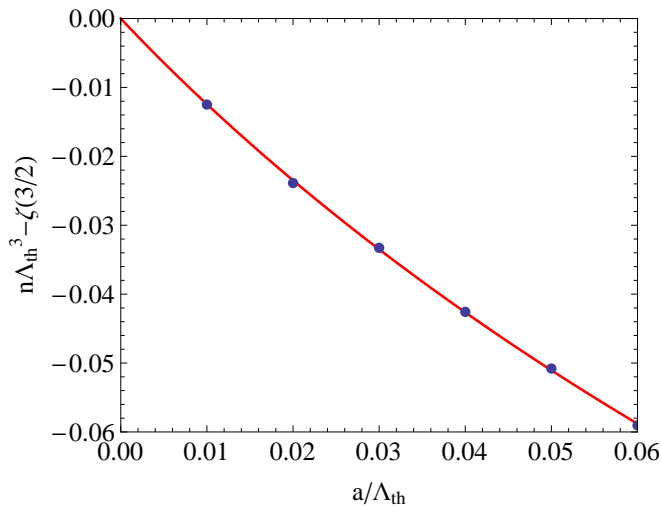


FIG. 12: Critical density shift due to interaction effect. The fitting line is $n\Lambda_{th}^3 - \zeta(3/2) = -1.3(a/\Lambda_{th}) - 2.1(a/\Lambda_{th})^2 \ln[(a/\Lambda_{th})]$.

of critical density due to interaction effects for one component Bose gases. We start with calculating the critical chemical potential $\mu_C = \Re[\hbar\Sigma(\mathbf{0}, 0)]$ for a given scattering length. Then we calculate the density at the critical chemical potential from $n = \int \frac{d\mathbf{k}}{(2\pi)^3} \int \hbar\omega N_B(\hbar\omega) \rho(\mathbf{k}, \omega)$. Fig.12 shows the lower critical density as the interaction strength is stronger. The calculation of a similar critical temperature shift from Renormalization Group calculation can be found in appendix B.

To gain more insight in the breakdown of the Boltzmann approach in the critical region, we consider the spectral function at low momentum inside (outside) the critical region, corresponding to the left (right) peak in

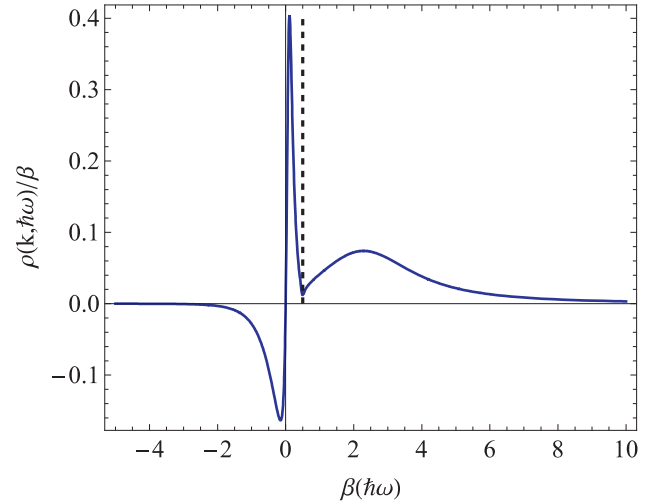


FIG. 13: Spectral function in one dimension (ignoring real part of selfenergy) at $k\Lambda_{th} = 0.1$ and $-\beta\mu = 0.5$. The vertical line indicates on-shell condition $\hbar\omega = \epsilon_{\mathbf{k}} - \mu$.

Fig. 10. The vertical lines correspond to $\epsilon_{\mathbf{k}} - \mu$. The peak in the spectral function is shifted considerably from its non-interacting value $\epsilon_{\mathbf{k}} - \mu$ in the critical region. Since the Boltzmann approach does not take into account the shifts in the quasi-particle energy beyond first order in the interaction it does not capture the shift in the critical region correctly. The latter is crucial for the divergence of the conductivity. The importance of the real part of the atomic self-energy in the critical region is also demonstrated by its importance in determining the upward shift in the critical temperature due to interactions, that is correctly found to be of order $\mathcal{O}(a/\Lambda_{th})^{19}$.

We have also calculated the spectral function in one dimension. We ignore the real part of selfenergy in the spectral function in this calculation. The spectral function in one dimension is shown in Fig. 13. The spectral function is exactly zero at on-shell condition. This is because of the contribution from the collision between particles with opposite momentum. This collision is responsible to the divergence of the imaginary part of the selfenergy and thus zero spectral function. We also note that the frequency sum-rule is not working here.

V. SCALING INVARIANCE AND CRITICAL EXPONENT

From the calculation that is based on the sunset diagram for the self-energy we find numerically that the spin conductivity diverges as $\sigma_s \sim 1/\sqrt{\mu_C - \mu}$. This result is understood on a more general level by considering scale invariance of the system. Near criticality, we have as a result of the simple (linearized) renormalization-group flow near the fixed point that the spectral function scales

as¹⁸

$$\rho(\lambda \mathbf{k}, \lambda^z \omega, \lambda^{1/\nu}(\mu - \mu_C)) = \frac{1}{\lambda^{2-\eta}} \rho(\mathbf{k}, \omega, \mu - \mu_C), \quad (25)$$

where λ is an arbitrary dimensionless scaling parameter and z , ν , and η are critical exponents. The relation between the correlation length ξ and the chemical potential is $\xi \sim 1/|\mu - \mu_C|^\nu$. From this scaling *ansatz* and Eq. (22) we find that $\sigma_s \sim \xi^{z-d+2-2\eta} \sim |\mu - \mu_C|^{-\nu(z-d+2-2\eta)}$, with d the number of spatial dimensions.

For the sunset diagram in three dimensions, we have $\nu = 1/2$, $z = 2$, and $\eta = 0$, in agreement with the numerical results. It is interesting to note that the behavior of the spin conductivity and the spin-drag relaxation time depends not only on the static critical exponents ν and η but also on the dynamical exponent z . We also note that, even though we ignored interactions between atoms with the same spin in our perturbative calculation based on the Feynman diagram in Fig. 8, the results based on the scaling *ansatz* are exact close to the critical temperature and do include these interactions.

Following the reasoning of Hohenberg and Halperin²⁰ the factor ξ^{2-d} in these results is understood as follows. A spin-dependent force acting on a region with (fluctuating) spin density n_s is balanced by viscous forces so that $n_s \xi^3 \mathbf{F} \sim \xi^3 \eta_v \mathbf{v}_s / \xi^2$, where \mathbf{v}_s is the spin velocity and η_v the viscosity. Using that $\mathbf{j}_s = n_s \mathbf{v}_s = \sigma_s \mathbf{F}$ this yields $\sigma_s \sim \xi^2 \langle n_s^2 \rangle / \eta_v$. We have that $\langle n_s^2 \rangle \sim \chi_s / \xi^{d20}$, with χ_s the spin susceptibility. In order to obtain full agreement with our result found from the scaling *ansatz* we thus need to have that the ratio $\chi_s / \eta_v \sim \xi^{z-2\eta}$. In future work we intend to investigate this conjecture in more detail.

VI. DISCUSSION AND CONCLUSIONS

We have incorporated the effect of critical fluctuations on the behavior of the spin-drag relaxation rate near the critical temperature for Bose-Einstein condensation. We found that the enhancement of the spin-drag relaxation rate due to Bose enhancement of interatomic interactions, predicted by the Boltzmann equation, is suppressed by critical fluctuations sufficiently close to the critical temperature. Numerically, we found the critical region to be proportional to the square of scattering length $|\Delta\mu| \approx 60(a/\Lambda_{\text{th}})^2$. An estimate based on the Ginzburg criterion²² confirms this result. Hence, the size of the critical region may be enlarged by increasing interatomic interactions near a Feshbach resonance. Furthermore, the Ginzburg criterion in d dimensions leads to $|\Delta\mu| \sim (a/\Lambda_{\text{th}})^{2/(4-d)}$. Reducing the dimensionality of the system therefore also increases the critical region. With respect to these remarks it is important to note that recent experiments with ultracold bosonic atoms have succeeded in accessing the critical region and measuring the exponent ν ²¹.

The spin conductivity and spin-drag relaxation rate can be measured directly in a drag measurement in which the two clouds of different spin feel a different force due a magnetic-field gradient. Another method is to study the damping of the spin-dipole mode that is fully determined by the spin-drag relaxation rate.

The main approximation leading to our results is to neglect vertex corrections in the evaluation of the spin-current spin-current response function. The Boltzmann equation is known to include vertex corrections that essentially lead to a replacement of the single-particle relaxation time by the appropriate transport relaxation time. In the absence of exact cancelations, which we do not expect to occur for the spin-drag conductivity, there is only a quantitative difference between these two time scales, and we attribute the difference between our Kubo approach and the Boltzmann approach sufficiently far away from the critical region to be due to this difference in time scales and hence to be due to neglecting vertex corrections. This assumption is strengthened by noting that far away from the critical region the Kubo and Boltzmann approach have qualitatively the same temperature dependence.

In this work we have considered the effect of thermal critical fluctuations since the phase transition to the Bose-Einstein-condensed state takes place at nonzero temperature. An interesting direction for future work is to investigate also the influence of the vicinity of a quantum critical point²³ on spin transport in Bose gases, for example by considering the system in an optical lattice where the Mott-insulator-to-superfluid quantum phase transition occurs²⁴. An additional interesting feature of this system is that due to the presence of the optical lattice, which breaks Galilean invariance, now also charge (mass) transport can be considered.

Acknowledgments

This work was supported by a Huygens Scholarship, the Stichting voor Fundamenteel Onderzoek der Materie (FOM), the Netherlands Organization for Scientific Research (NWO), and by the European Research Council (ERC) under the Seventh Framework Program (FP7). We would like to thank Hedwig van Driel and Vivian Jacobs for their help with the calculations.

Since this paper is also Rakpong's thesis, here is Rakpong's acknowledgement: "During my study here in Utrecht, I have got two financial supports, Utrecht Excellence Scholarship and Huygens Scholarship. I would like to express my gratitude here. It is impossible for me to even start this thesis without these scholarships. I am also very fortunate to have two supervisors for this thesis. It is hard to imagine having supervisors better than Henk and Rembert. They are complementary to each other. Henk is experienced in cold-atom systems. He is the one who I can undoubtedly call a physicist. By a physicist, I mean the one who use physical argu-

ments and physical pictures to understand nature in addition to mathematics, simulations and/or experiments. Furthermore, he always looks happy when talking about physics. This is important for a student like me who have to gather my courage everytime before going to a professor. Rembert specializes in spintronics. He always helps me see the better big picture of the project. This is helpful for inexperienced students who can easily get lost in the vast field of knowledge. He also helps me in the detail like a nasty problem of “Where’s my minus sign?”. Moreover, both of them never get angry when I did stupid mistakes. I feel like “a level up!” after working with them for one year. I also want to thank all of my friends here. Among them, the most notable is Jougundas. He helps me from the start to the end, from the most trivial things like correcting my poor English to the complicated things like running Mathematica from the server. My study here would be much harder without him. I also want to thank my girlfriend, Wisuttida, for continuous support. Lastly, I am what I am capable of mostly because of my parents. I profoundly thank them here.”

APPENDIX A: SELFENERGY FROM MANY-BODY TRANSITION MATRIX

In this section we give another example of the selfenergy. It is the selfenergy from many-body T matrix in the limit where the external momentum and external frequency of T matrix is zero and small, respectively. We start with the expression for many-body T matrix with zero external momentum

$$\begin{aligned} \frac{1}{T^{MB}(i\hbar\omega_n)} &= \frac{1}{V_0} - \int \frac{d\mathbf{k}}{(2\pi)^3} \frac{1 + 2N(\epsilon_{\mathbf{k}})}{i\hbar\omega_n - 2(\epsilon_{\mathbf{k}} - \mu)} \\ &= \frac{1}{V_0} - \Xi_1(0, i\omega_n) - \Xi_2(0, i\omega_n), \quad (\text{A1}) \end{aligned}$$

with

$$\begin{aligned} \Xi_1(0, i\omega_n) &= \int \frac{d\mathbf{k}}{(2\pi)^3} \frac{1}{i\hbar\omega_n - 2(\epsilon_{\mathbf{k}} - \mu)} \\ &\quad \times \left(i + 2N(\epsilon_{\mathbf{k}}) - \frac{2}{\beta(\epsilon_{\mathbf{k}} - \mu)} \right) \\ \Xi_2(0, i\omega_n) &= \int \frac{d\mathbf{k}}{(2\pi)^3} \frac{1}{i\hbar\omega_n - 2(\epsilon_{\mathbf{k}} - \mu)} \frac{2}{\beta(\epsilon_{\mathbf{k}} - \mu)}. \quad (\text{A2}) \end{aligned}$$

The term $\Xi_1(0, i\omega_n)$ is finite when $\omega_n \rightarrow 0$, so we approximate this term to be a constant and absorb it into V_0 . Another term $\Xi_2(0, i\omega_n)$ has infrared divergence and has to be treated carefully. Fortunately, the momentum integral can be evaluated analytically, it yields

$$\Xi_2(0, i\hbar\omega_n) = \frac{m^{\frac{3}{2}}}{\beta\hbar^3\pi} \left(\frac{\sqrt{-i\hbar\omega_n - 2\mu} - \sqrt{-2\mu}}{i\hbar\omega_n} \right). \quad (\text{A3})$$

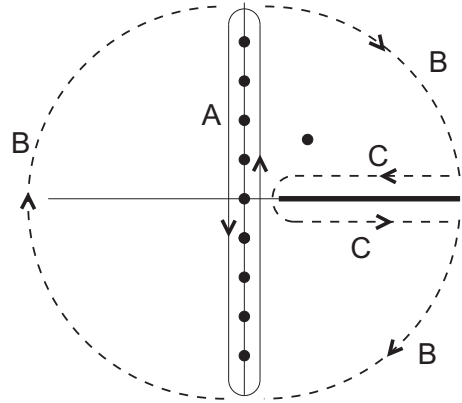


FIG. 14: Illustration of contour integration for calculating selfenergy.

The selfenergy follows from closing the external lines of the T matrix

$$\hbar\Sigma(i\omega_n) = -\frac{1}{\hbar\beta} \int \frac{d\mathbf{k}}{(2\pi)^3} \sum_m [T^{MB}(0, i\omega_m + i\omega_n) \times G(\mathbf{k}, i\omega_m)] \quad (\text{A4})$$

The matsubara summation can be converted into contour integral. The analytic structure of this integrand is shown in Fig.14. Both branchcut and pole contribute to the result

$$\begin{aligned} \text{Im}[\hbar\Sigma^+(\omega)] &= \int_{\epsilon_{\mathbf{k}}=-\hbar\omega-\mu}^{\epsilon_{\mathbf{k}}=\infty} \frac{d\mathbf{k}}{(2\pi)^3} [N(\hbar\omega + \epsilon_{\mathbf{k}} - \mu) - N(\epsilon_{\mathbf{k}} - \mu)] \frac{\hbar^3\pi\beta}{m^{3/2}} \\ &\quad \frac{(\hbar\omega + \epsilon_{\mathbf{k}} - \mu)\sqrt{\hbar\omega + \epsilon_{\mathbf{k}} + \mu}}{\left[\frac{1}{V_0} \frac{\beta\hbar^3\pi}{m^{3/2}} (\hbar\omega + \epsilon_{\mathbf{k}} - \mu) + \sqrt{-2\mu} \right]^2 + (\hbar\omega + \epsilon_{\mathbf{k}} + \mu)} \quad (\text{A5}) \end{aligned}$$

APPENDIX B: RENORMALIZATION GROUP CALCULATION FOR CRITICAL TEMPERATURE SHIFT

Renormalization Group is a powerful tool for studying scale invariant system. The idea of renormalization group is to calculate effective hamiltonian at macroscopic scale by integrating out short wavelength degree of freedom. Because of scale invariance, the form of hamiltonian remains unchange but some parameters will change when we integrate out short wavelength degree of freedom. These parameters are called running parameters and the equations describing the change of these parameter are called flow equations. In the system of Bose gas,

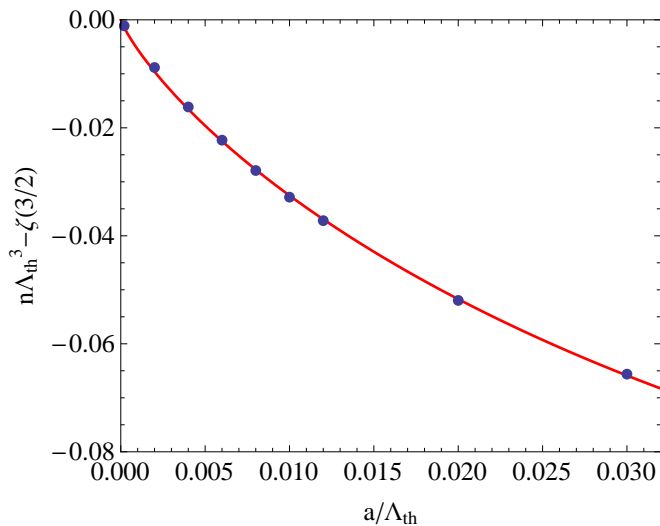


FIG. 15: The shift in critical density due to interaction effect. The fitted line is $n\Lambda_{th}^3 - \zeta(3/2) = -(a/\Lambda_{th}) \ln(0.3(\Lambda_{th}/a))$.

the most important running parameters are chemical potential μ and interaction strength V_0 . The flow equations for these two parameters are²⁵

$$\begin{aligned} \frac{d\mu(l)}{dl} &= 2\mu(l) - V_0(l) \frac{\Lambda(l)^3}{\pi^2} N_B(\epsilon_{\Lambda(l)} - \mu(l)) \\ \frac{dV_0(l)}{dl} &= -V_0(l) - V_0(l)^2 \frac{\Lambda(l)^3}{2\pi^2} \left\{ \frac{1 + 2N_B(\epsilon_{\Lambda(l)} - \mu(l))}{2(\epsilon_{\Lambda(l)} - \mu(l))} \right. \\ &\quad \left. + 4\beta(l)N_B(\epsilon_{\Lambda(l)} - \mu(l))[N_B(\epsilon_{\Lambda(l)} - \mu(l)) + 1] \right\}. \end{aligned} \quad (B1)$$

Here l is the parameter that runs from zero to infinity as we integrate wavevector Λ . The relation between them is $\Lambda(l) = \Lambda e^{-l}$. The running parameters in above equation are scaled with $\mu(l) = \mu e^{2l}$, $V_0(l) = V_0 e^{2l}$ and $\beta(l) = \beta e^{-2l}$. The critical density can be calculated from $n = \int \frac{d\mathbf{k}}{(2\pi)^3} N(\epsilon_{\mathbf{k}} - \mu) \frac{\partial \mu}{\partial \mu(l=0)}$ where we have to select $\mu(l=0)$ such that $\mu(l \rightarrow \infty) = 0$. The effect of repulsive interaction on critical density is shown in Fig.15.

APPENDIX C: HEAT TRANSPORT AND "FIGURE OF MERIT"

In addition to spin current induced by external forces, temperature gradients can also drive the spin current. Similarly, heat current can be driven by both external forces and temperature gradients. There are four transport coefficients in total. They are best illustrated in

term of the matrix

$$\begin{bmatrix} J_S \\ J_Q \end{bmatrix} = \begin{bmatrix} \sigma_s & S\sigma_s \\ S\sigma_s T & \kappa' \end{bmatrix} \begin{bmatrix} F \\ -\nabla T \end{bmatrix}. \quad (C1)$$

In the above expression, J_S and J_Q are spin current and heat current, respectively. Furthermore, S is called Seebeck coefficient and κ' is the thermal conductivity at zero external force. The calculation of $S\sigma_s$ and κ' can be done by adding the term $(\epsilon_{\mathbf{k}} - \mu)/T$ and $(\epsilon_{\mathbf{k}} - \mu)(\epsilon_{\mathbf{k}} - w)/T$ to Eq. (22), respectively. Here $\mu = \mu_C - A\xi^{-1/\nu}$ and $w = \mu_C - B\xi^{-\alpha}$ is enthalpy with α assumed to be positive and A, B constants. At critical point where correlation length diverges, $S\sigma_s = -\sigma_s \mu_C / T$ and $\kappa' = \sigma_s \mu_C^2 / T$. We introduce a quantity $Z' = \sigma_s S^2 / \kappa'$. In this case, we find $Z'T = 1$ at critical point. We also introduce figure of merit $Z = \sigma_s S^2 / \kappa' (1 - Z'T) = Z' / (1 - Z'T)$, an important quantity in material science. Materials with high figure of merit is important in technological applications. Our calculation suggests that $ZT \rightarrow \infty$ as we go to the critical point. To calculate the critical exponent of figure of merit, we rewrite Eq. (22) as $\sigma_s = \xi^{z-d+2-2\eta} \int dx dy f(\mathbf{x}, y)$ with $x = k\xi$ and $y = \omega\xi^z$. The Seebeck coefficient is then

$$S = (\xi^{-2} \langle \epsilon_x \rangle + A\xi^{-1/\nu} - \mu_C) \frac{1}{T}, \quad (C2)$$

with $\langle \dots \rangle = \frac{\int dx dy (\dots) f(\mathbf{x}, y)}{\int dx dy f(\mathbf{x}, y)}$. The thermal conductivity can be calculated in the same way

$$\kappa' = \langle (\xi^{-2} \epsilon_x + A\xi^{-1/\nu} - \mu_C)(\xi^{-2} \epsilon_x + B\xi^{-\alpha} - \mu_C) \rangle \frac{\sigma_s}{T^2}. \quad (C3)$$

From this, we calculate the critical exponent of $1 - Z'T$ and also the exponent of Z . Assuming $1/\nu > 0.5$, we now separate the calculation into three cases. Case I: $1/\nu > \alpha$,

$$\begin{aligned} Z'T &\approx \frac{\mu_C^2 - 2A\xi^{-1/\nu} \mu_C}{\mu_C^2 - B\xi^{-\alpha} \mu_C} \\ &\approx 1 + \frac{B}{\mu_C} \xi^{-\alpha} \\ 1 - Z'T &\approx -\frac{B}{\mu_C} \xi^{-\alpha}. \end{aligned} \quad (C4)$$

Thus the figure of merit $Z \sim \xi^\alpha$. Case II: $1/\nu < \alpha$, in the same spirit as the above calculation we found $1 - Z'T \approx \frac{A}{\mu_C} \xi^{-1/\nu}$ and $Z \sim \xi^{1/\nu}$. Case III: $\mu = w$, we found $1 - Z'T \approx \frac{\xi^{-4}}{\mu_C^2} (\langle \epsilon_x^2 \rangle - \langle \epsilon_x \rangle^2)$ and thus $Z \sim \xi^4$.

¹ S. A. Wolf, D. D. Awschalom, R. A. Buhrman, J. M. Daughton, S. von Molnár, M. L. Roukes, A. Y. Chtchelka-

nova and D. M. Treger, Science **294**, 1488 (2001).
² Shuichi Murakami, Naoto Nagaosa, and Shou-Cheng

- Zhang, *Science* **301**, 1348 (2003).
- ³ Jairo Sinova, Dimitrie Culcer, Q. Niu, N. A. Sinitsyn, T. Jungwirth, and A. H. MacDonald, *Phys. Rev. Lett.* **92**, 126603 (2004).
- ⁴ I. D'Amico and G. Vignale, *Phys. Rev. B* **62**, 4853 (2000).
- ⁵ C. P. Weber, N. Gedik, J. E. Moore, J. Orenstein, J. Stephens and D. D. Awschalom, *Nature* **437**, 1330 (2005).
- ⁶ H.T.C. Stoof, K.B. Gubbels, D.B.M. Dickerscheid *Ultracold Quantum Fields*, (Springer, Dordrecht, 2009)
- ⁷ J.C. Slonczewski, *J. Magn. Magn. Mater.* **159**, L1 (1996).
- ⁸ L. Berger, *Phys. Rev. B* **54**, 9353 (1996).
- ⁹ M. Tsoi, A. G. M. Jansen, J. Bass, W.-C. Chiang, M. Seck, V. Tsoi, and P. Wyder, *Phys. Rev. Lett.* **80**, 4281 (1998).
- ¹⁰ E. B. Myers, D. C. Ralph, J. A. Katine, R. N. Louie, R. A. Buhrman, *Science* **285**, 867 (1999).
- ¹¹ M.E. Fisher and J.S. Langer, *Phys. Rev. Lett.* **20**, 665 (1968).
- ¹² R.A. Duine and H.T.C. Stoof, *Phys. Rev. Lett.* **103**, 170401 (2009).
- ¹³ M. Polini and G. Vignale, *Phys. Rev. Lett.* **98**, 266403 (2007); Diego Rainis, Marco Polini, M. P. Tosi, and G. Vignale, *Phys. Rev. B* **77**, 035113 (2008).
- ¹⁴ G. M. Bruun, A. Recati, C. J. Pethick, H. Smith, and S. Stringari, *Phys. Rev. Lett.* **100**, 240406 (2008).
- ¹⁵ S. Riedl, E. R. Sánchez Guajardo, C. Kohstall, A. Altmeyer, M. J. Wright, J. Hecker Denschlag, R. Grimm, G. M. Bruun, and H. Smith, *Phys. Rev. A* **78**, 053609 (2008).
- ¹⁶ R. A. Duine, Marco Polini, H. T. C. Stoof, and G. Vignale, *Phys. Rev. Lett.* **104**, 220403 (2010).
- ¹⁷ H.J. van Driel, R.A. Duine, and H.T.C. Stoof, *Phys. Rev. Lett.* **105**, 155301 (2010).
- ¹⁸ D. J. Amit, *Field Theory, the Renormalization Group, and Critical Phenomena*, (World Scientific, London, 1978).
- ¹⁹ Gordon Baym, Jean-Paul Blaizot, Markus Holzmann, Franck Laloë, and Dominique Vautherin, *Phys. Rev. Lett.* **83**, 1703 (1999).
- ²⁰ P.C. Hohenberg and B.I. Halperin, *Rev. Mod. Phys.* **49**, 435 (1977).
- ²¹ T. Donner, S. Ritter, T. Bourdel, A. Ött, M. Köhl, and T. Esslinger, *Science* **315**, 5818 (2007)
- ²² V.L. Ginzburg, *Sov. Phys. Solid State* **1**, 1824 (1960).
- ²³ Kedar Damle and Subir Sachdev, *Phys. Rev. B* **56**, 8714 (1997).
- ²⁴ M. Greiner, O. Mandel, T. Esslinger, T. W. Hänsch, and I. Bloch, *Nature* **415**, 39 (2002).
- ²⁵ M. Bijlsma and H.T.C. Stoof, *Phys. Rev. A* **54**, 5085 (1996).